Neural Networks and Gaussian Regression Process Comparison on a Physical Problem

Merve Gurbuz-Caldag[1], Bengisen Pekmen[1], and Ezgi Kiratli[2(✉)]

[1] Department of Mathematics, TED University, 06420 Ankara, Turkey
merve.gurbuz@tedu.edu.tr
[2] Department of Economics, TED University, 06420 Ankara, Turkey
ezgi.kiratli@tedu.edu.tr

Abstract. This study aims to systematically compare two machine learning methods, Gaussian Process Regression (GPR) and Neural Networks (NN), for predicting heat transfer, mass transfer, and microbial behavior indicators in a bioconvection flow problem. The models are trained and tested on a dataset collected from numerical simulation results of the natural bioconvection flow of a Cu-water nanofluid and oxytactic bacteria in an open square cavity. Radial basis function method is performed by parallel computing in different dimensionless problem parameters. The target variables, average Nusselt, Sherwood and bacteria density are computed in each parameter combinations. Multiple seed comparison, cross validation analysis and permutation based feature importance analysis were carried by both models. The results reveal that in terms of mean squared error (MSE) metrics, in different seeds, GPR is more robust to model, and in turn measure uncertainty well while NN is provides smaller prediction error. 5 fold CV analysis results approve the good generalizability of NN model. Permutation based feature importance check shuffling each input data and controlling MSE values points to the most important parameter as bioconvection Rayleigh number on each output indicator.

Keywords: Neural Networks · Gaussian Process Regression · Radial Basis Function Method

1 Introduction

Bioconvection originates from the collective upward swimming of motile microorganisms, which generates density gradients and induces convective instability within the fluid. The theoretical foundations and pattern formation mechanisms of bioconvection were comprehensively discussed by Hill and Pedley [14]. Subsequent studies demonstrated that thermal gradients significantly affect the onset of thermo-bioconvective instability in porous layers [19]. The incorporation of nanoparticles into microorganism suspensions further modifies the stability characteristics due to Brownian motion and thermophoretic effects, altering the critical conditions for nanofluid bioconvection [18,20]. In addition, the presence of non-Darcian porous media and gyrotactic microorganisms has been shown to influence flow destabilization and transport enhancement

© The Author(s), under exclusive license to Springer Nature Switzerland AG 2027
O. Gervasi et al. (Eds.): ICCSA 2026, LNCS 16768, pp. 464–475, 2027.
https://doi.org/10.1007/978-3-032-30488-9_29

[27]. More recently, thermo-bio-convection in complex porous cavities containing nanoparticles and microorganisms has been numerically investigated, revealing strong coupling between thermal, concentration, and microorganism fields [1,3].

Open cavities are widely used in a range of engineering applications, including solar thermal receivers, convective heat transfer from extended surfaces in heat exchangers, and solar collectors equipped with insulated strips [28]. Chan and Tien [6] studied the steady natural convection flow in an open cavity by using SIMPLER algorithm. They reported that higher Rayleigh number leads to the formation of recirculation zones above the bottom wall. Polat and Bilgen [24] analyzed laminar natural convection in inclined shallow open cavities heated by a constant heat flux. It is obtained that an asymptotic behaviour of heat transfer occurs as Rayleigh number increases. However, the elongation of open cavities postpones this behaviour. Mohamad et al. [23] simulated natural convection in an open-ended cavity using the Lattice Boltzmann Method (LBM) and examined the associated flow and heat transfer characteristics. Their results confirmed the reliability of the open boundary conditions by showing close agreement with finite volume method predictions, and revealed that increasing the cavity aspect ratio leads to an asymptotic decrease in the heat transfer rate toward the conduction limit. LBM is applied to solve natural convection flow in an open cavity filled with Cu-water by Kefayati et al. [16]. Gangawane [11] showed that the magnetic field orientation strongly affects heat transfer of natural convection in an open ended cavity with partiallyactive walls. Prakash et al. [25] conducted MHD free convection in a partially open square cavity with a wavy cold wall filled with nanofluid. They reported that increasing the Hartmann number or nanoparticle volume fraction suppresses convection, whereas wall waviness enhances the average Nusselt number. Allouche et al. [2] developed an in-house FORTRAN code to numerically investigate two-dimensional laminar natural convection of a Newtonian nanofluid in an open square cavity subjected to an external magnetic field. It is shown that stronger magnetic fields suppress fluid motion and heat transfer, whereas the inclusion of nanoparticles enhances heat transfer and alters the flow behavior depending on the presence of the magnetic field.

In recent years, the machine learning approaches on convective heat transfer of nanofluid problems in different geometries are studied by many researchers. Vaferi et al. [31] developed a model to forecast the heat transfer coefficient of nanofluids in a circular tube. The proposed model is compared with different ANN types using experimental data. Rostamian et al. [26] proposed ANN model and correlation of the thermal conductivity (TC) of CuO-SWCNTs/EG water. They deduced that ANN model gives more accurate results than the correlation. The effect of number of neurons in hidden layers on the ANN prediction for TC of hybrid nanofluids is analyzed by Vafei et al. [30]. In [29], the Sherwood number, motile density of microorganism, skin friction coefficient and Nusselt number are predicted using four different artificial neural network models. Chandra and Das [7] conducted a study on ANN model for the estimation of gyrotactic-nanofluid flow over a stretchable vertically inclined surface. In [15], the average Nusselt, Sherwood and motile microorganism numbers of the mixed bioconvection flow of nanofluid of oxytactic bacteria through a porous cavity under the effect of periodic magnetic field is modeled using Light Gradient Boosting Machine algorithm.

To the best of our knowledge, NN and GPR modeling on a bioconvection flow in an open square cavity filled by Cu-water nanofluid in the presence of oxytactic bacteria is firstly conducted. The dimensionless governing equations are formulated in terms of stream function, vorticity, temperature, oxygen concentration and bacteria density, and solved numerically using the RBF method. Considering various combinations of dimensionless parameters including the Rayleigh, bioconvection Rayleigh, Hartmann, magnetic, Lewis and Peclet numbers as well as the magnetic source location, the target outputs the average Nusselt number, Sherwood number and bacteria density along the heated wall are computed, and all are saved. The predictive performances of the models are evaluated using this dataset. To the best of our knowledge, this is the first study to apply and systematically compare NN and GPR modeling to a bioconvection problem in an open cavity.

The motivation of this study arises from the growing need for data-driven models, where repetitive numerical simulations are computationally expensive. While neural networks are widely adopted due to their predictive power, Gaussian Process Regression including Kernels as in our numerical method is also examined. A systematic comparison of these two approaches on a well-defined physical problem is utilized. The objectives of this work are: (i) to construct a high-quality dataset from RBF-based numerical simulations of bioconvection flow in an open cavity, (ii) to train and evaluate NN and GPR models on this dataset using multiple performance metrics, and (iii) to provide guidance on model selection based on accuracy, generalizability, and computational cost.

2 Physics of the Problem

Under steady-state conditions, natural convection flow of Cu-water nanofluid in a square cavity, taking into account the presence of oxytactic bacteria and the influence of a magnetic source is concerned. The setup of the problem is illustrated in Fig. 1. The location of magnetic source (ms) is denoted by (xms, yms).

The single-phase model is adopted for the nanofluid, and accordingly, its physical properties are defined by [17]

$$\rho_{nf} = (1-\xi)\rho_f + \xi\rho_s, \tag{1}$$

$$(\rho c_p)_{nf} = (1-\xi)(\rho c_p)_f + \xi(\rho c_p)_s, \tag{2}$$

$$(\rho\beta)_{nf} = (1-\xi)(\rho\beta)_f + \xi(\rho\beta)_s, \tag{3}$$

$$\alpha_{nf} = \frac{k_{nf}}{(\rho c_p)_{nf}}, \tag{4}$$

where subindices nf, f, s are the nanofluid, fluid and solid, respectively, ρ is the density, β is the thermal expansion coefficient, c_p is the specific heat, α is the thermal diffusivity and ξ is the solid volume fraction. The thermal (k_{nf}) and electrical σ_{nf} conductivities

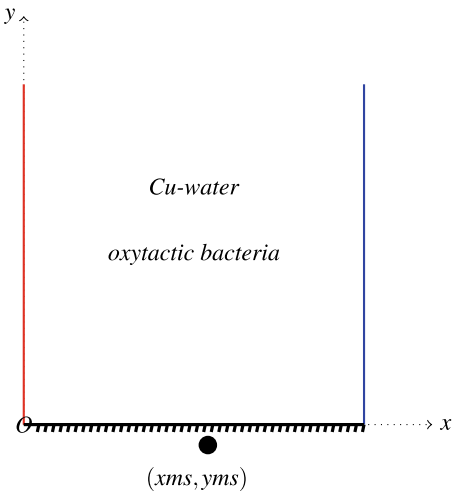

Fig. 1. The geometrical layout of the problem.

of the nanofluid are settled as [12]

$$\frac{k_{nf}}{k_f} = \frac{k_s + 2k_f - 2\xi(k_f - k_s)}{k_s + 2k_f + \xi(k_f - k_s)}, \tag{5}$$

$$\frac{\sigma_{nf}}{\sigma_f} = \frac{\sigma_s + 2\sigma_f - 2\xi(\sigma_f - \sigma_s)}{\sigma_s + 2\sigma_f + \xi(\sigma_f - \sigma_s)}, \tag{6}$$

and the dynamic viscosity of nanofluid μ_{nf} is opted as [5]

$$\mu_{nf} = \mu_f(1-\xi)^{-2.5}. \tag{7}$$

Table 1 summarizes the thermophysical properties of water and copper (Cu).

Table 1. Thermophysical properties of water and Copper (Cu) [4,13].

Property	Water	Cu
$\rho\ (kg/m^3)$	997.1	8933
$c_p\ [J/(kgK)]$	4179	385
$k\ [W/(mK)]$	0.613	401
$\beta \times 10^{-5}\ (1/K)$	21	1.67
$\sigma\ (1/(m\Omega))$	0.05	5.96×10^7

By using the stream function to define the velocity components, $\nabla \cdot (u, v) = 0$ is satisfied. Additionally, introducing vorticity eliminates the pressure terms from the momentum equations. As a result, the governing equations are reformulated in terms

of stream function (ψ), vorticity (ω), temperature (T), oxygen concentration (C) and the density of the bacteria (N_m) as follows:

$$\nabla^2\psi = -\omega, \tag{8a}$$

$$\frac{\alpha_{nf}}{\alpha_f}\nabla^2 T = \left(u\frac{\partial T}{\partial x} + v\frac{\partial T}{\partial y}\right), \tag{8b}$$

$$\frac{1}{Le}\nabla^2 C = \left(u\frac{\partial C}{\partial x} + v\frac{\partial C}{\partial y}\right) + \frac{1}{Le}N_m, \tag{8c}$$

$$\frac{1}{Le}\nabla^2 N_m = \left(u\frac{\partial N_m}{\partial x} + v\frac{\partial N_m}{\partial y}\right) + \frac{Pe}{Le}\left(N_m\nabla^2 C + \frac{\partial C}{\partial x}\frac{\partial N_m}{\partial x} + \frac{\partial C}{\partial y}\frac{\partial N_m}{\partial y}\right), \tag{8d}$$

$$\begin{aligned}\frac{\mu_{nf}}{\mu_f}Pr\nabla^2\omega = {} & \frac{\rho_{nf}}{\rho_f}\left(u\frac{\partial\omega}{\partial x} + v\frac{\partial\omega}{\partial y}\right) - RaPr\left(\frac{(\rho\beta)_{nf}}{\rho_f\beta_f}\frac{\partial T}{\partial x} - Rb\frac{\partial N_m}{\partial x}\right) - \\ & MnFPr\left(\frac{\partial H}{\partial x}\frac{\partial T}{\partial y} - \frac{\partial H}{\partial y}\frac{\partial T}{\partial x}\right) + \frac{\sigma_{nf}}{\sigma_f}Ha^2Pr\Big[H_x^2 v_x - H_x H_y(u_x - v_y) - H_y^2 u_y \\ & + 2H_x H_{xdx}v - H_{xdx}H_y u - H_x H_{ydx}u - 2H_y H_{ydy}u + H_{xdy}H_y v + H_x H_{ydy}v\Big],\end{aligned} \tag{8e}$$

where $H_{xdx}, H_{xdy}, H_{ydx}, H_{ydy}$ are partial derivatives of $H_x = |yms|\dfrac{y-yms}{(x-xms)^2+(y-yms)^2}$ and $H_y = |yms|\dfrac{xms-x}{(x-xms)^2+(y-yms)^2}$, and $H = \sqrt{H_x^2+H_y^2}$. The nondimensional parameters are Prandtl, Hartmann, Rayleigh, bioconvection Rayleigh, Lewis, Peclet and magnetic numbers given as

$$Pr = \frac{\nu_f}{\alpha_f},\ Ha = L\mu_0 H_0\sqrt{\frac{\sigma_f}{\mu_f}},\ Ra = \frac{g\beta_f L^3\Delta T}{\alpha_f\nu_f}, \tag{9a}$$

$$R_b = \frac{\gamma\Delta\rho n_0}{\rho_f\beta_f\Delta T},\ \ Pe = \frac{\tilde{b}W_c}{D_n},\ \ Le = \frac{\alpha_f}{D_c},\ \ MnF = \frac{\mu_0 H_0^2\tilde{K}\Delta T L^2}{\mu_f\alpha_f} \tag{9b}$$

where ν is the kinematic viscosity, g is the gravitational acceleration, γ is the mean volume of microorganism, D_c is the diffusivity of oxygen concentration, W_c is the maximum cell swimming speed, $\tilde{b}$ is the chemotaxis constant, D_n is the diffusivity of microorganism, L is the characteristic length, n_0 is the average density of bacteria, μ_0 is the magnetic permeability, H_0 is the intensity of the magnetic field, $\tilde{K}$ is a constant, ΔT is the temperature difference and $\Delta\rho = \rho_{cell} - \rho_{nf}$. Boundary conditions are as follows

$$\begin{aligned}&\text{on } x = 0 : u = v = \psi = 0, T = 1, C = N_m = 1,\\ &\text{on } x = 1 : u = v = \psi = 0 = T, C = N_m = 1,\\ &\text{on } y = 0 : u = v = \psi = 0, \frac{\partial T}{\partial y} = 0, C = 1, PeN_m\frac{\partial C}{\partial y} = \frac{\partial N_m}{\partial y},\\ &\text{on } y = 1 : \frac{\partial C}{\partial y} = \frac{\partial N_m}{\partial y} = \frac{\partial\psi}{\partial y} = 0, \quad \begin{cases}\dfrac{\partial T}{\partial y} = 0 & \text{if } v \geq 0\\ T = 0 & \text{if } v < 0\end{cases}.\end{aligned}$$

3 Computational Approaches

3.1 Radial Basis Function (RBF) Method

The numerical part of the study is carried out by applying the global radial basis function (RBF) method to space derivatives.

RBFs are functions depending on the radial (Euclidean) distance $r = \sqrt{(x-x_j)^2+(y-y_j)^2}$ between the collocation (x_j, y_j) and the field (x, y) points. The novel and concise books [9, 10] involve many theoretical and practical implementation examples on RBFs.

Any unknown φ may be written as a product of a coordinate matrix F constructed by an RBF and an unknown vector of coefficients. The partial derivatives of unknown is also easily derived by this product and by the straightforward derivative calculations of RBFs. The differentiation matrices for x-, y- derivatives and Laplacian are found as

$$D_x = \frac{\partial F}{\partial x}F^{-1}, D_y = \frac{\partial F}{\partial y}F^{-1}, D_2 = \left(\frac{\partial^2 F}{\partial x^2} + \frac{\partial^2 F}{\partial y^2}\right)F^{-1}, \tag{10}$$

Iterations are terminated if the sum of the relative residuals in infinity norm is less than a tolerance 10^{-5}. A relaxation parameter $\tau\,(0 < \tau < 1)$ is utilized once ω equation is solved.

Average Nusselt and Sherwood numbers, and density of the bacteria along the heated wall are computed by

$$\overline{Nu} = -\frac{k_{nf}}{k_f}\int_0^1 \frac{\partial T}{\partial x}dy,\ \overline{Sh} = -\int_0^1 \frac{\partial C}{\partial x}dy,\ \overline{Nm} = -\int_0^1 \frac{\partial N_m}{\partial x}dy, \tag{11}$$

using composite Simpson's rule on uniform grids.

3.2 Machine Learning Techniques

Neural Network Regression. NN process works as feedforward NN [8]. In this case, the information flows from the left to the right. The first layer is the input layer. The hidden layers follow the first layer, and the last layer is the output layer. A simple generalized mathematical expression may be written as

$$\hat{\mathbf{y}} = f(W\mathbf{x} + b), \tag{12}$$

where W is the weight matrix, b is the bias vector, $\mathbf{x}$ is the input features, $\hat{\mathbf{y}}$ is the predicted output, and f is the activation function.

In MATLAB, 'fitrnet' is used for NN modeling.

Gaussian Process Regression (GPR). In this process kernel (covariance) functions play the significant role. The GP function $f(x)$ is expressed as [21]

$$f(x) \approx GP(m(x), k(x, x')), \tag{13}$$

where $m(x) = E[f(x)]$ is the mean function, $k(x,x') = E[(f(x) - m(x))(f(x') - m(x'))]$ is the covariance function. In this study, ARD squared exponential kernel is taken as

$$k(x,x') = \sigma^2 \exp\left[-\frac{1}{2} \sum_{m=1}^{d} \frac{(x_m - x'_m)^2}{\sigma_l^2} \right], \tag{14}$$

where σ is the standard deviation, σ_l is the characteristic length scale, x, x' are input vectors of size $d \times 1$.

In MATLAB, 'fitrgp' is used for GP modeling.

4 Machine Learning Modeling

In this part, bilayer NN and GPR modeling results obtained in MATLAB are to be compared. All computations were carried out in MATLAB R2025a [22].

The RBF method iteratively solves the non-dimensional equations Eqs. (8)). The data is collected from the numerical results in different combination of dimensionless parameters which are in the range:

$$\begin{aligned}
Ra &= [10^2, 500, 10^3, 5000, 10^4];\\
Rb &= [10, 20, 30, 40, 50];\\
Ha &= [10, 35, 50, 100];\\
MnF &= [25, 50, 100];\\
xms &= [0.1, 0.25, 0.5, 0.75, 0.9];\\
yms &= [-0.02, -0.04, -0.08].
\end{aligned}$$

In numerical executions, the relaxation parameter is fixed at 0.002 for all $Ha <= 50$ cases while it is assigned as 0.0005 at $Ha = 100$. The convergent 2679 results are stored, and used for modeling. Thus, the dataset has 6 columns with input features $Ra, Rb, Ha, MnF, xms, yms$ and 3 columns with output features $\overline{Nu}, \overline{Sh}, \overline{N_m}$ In the case of NN modeling, hidden layer size is fixed at 50 neurons in each layer.

Different seeds affect the train-validation data split and the randomness in both the initial network weights inn NN. Since both factors influence model performance, we tested multiple seeds to identify which combination yields the best results. This approach helps us to avoid selecting a model that performs well simply due to a fortunate random configuration.

In Table 2, a comparison of bilayer NN and GPR with various kernel functions is conducted across random seeds between 20 and 50 using an 80%/20% train/test split. The target variable is the average Nusselt number ($\overline{Nu}$) which is difficult one to predict. Mean MSE refers to the average of MSE test values found in each seed. Std indicates the how much MSE test values deviates from the mean MSE. The smallest deviation points to a more consistent and robust model. Best MSE is the minimum test error achieved among all seeds. Best Seed is the specific random seed that produced the minimum test error. According to the Table results, the best models having the best MSE less than 0.001 are found in seed 28. The smallest mean MSE is obtained by NN modeling. The small variability in GPR-ARD-SE also gives us a robust modeling

tool. To further benchmark our two methods against other established ML techniques, Random Forest (100 trees, minimum leaf size of 5) and XGBoost via LSBoost (1000 cycles, learning rate of 0.1, maximum splits of 20) were also evaluated under the same seed and split conditions. As seen in the last two rows of the Table, both ensemble methods yield competitive but inferior performance compared to the leading models. NN retains the smallest mean MSE overall, confirming its suitability as the primary modeling tool for predicting $\overline{Nu}$ in this problem. Since the primary objective of this study is the comparison of NN and GPR, exhaustive tuning of these ensemble methods beyond the scope of this work.

Table 2. Model performance across 31 random seeds (20–50)

Model	Mean MSE	Std	Best MSE	Best Seed
NN	**0.000487**	0.000304	**0.000113**	28
GPR-ARD-SE	0.000531	*0.000235*	*0.000184*	28
GPR-Squared Exponential	0.000841	*0.000235*	0.000400	28
GPR-Rational Quadratic	0.000848	0.000237	0.000400	28
GPR-Matérn 5/2	0.001787	0.000364	0.001007	28
GPR-Matérn 3/2	0.003957	0.000738	0.002839	44
RF	0.033306	0.002921	0.028427	32
XGBoost	0.000641	0.000268	0.000215	28

The prediction and residual plots are also displayed in Fig. 2. Both modeling capture the prediction in a very good pattern. Regarding three separate modeling for three outputs, NN modeling is completed in 6 s while total GPR modeling duration is 106 s.

5 folds cross validation (CV) analysis is also examined with both models keeping seed at 28. CV allows us to understand how well the models generalize to new data, giving a more reliable performance estimate than a single train-test split. By keeping the seed fixed, both models are trained and tested on exactly the same data partitions, which makes the comparison fair. In this approach, the dataset is divided into 5 subsets, and each subset takes a turn being the test set while the other 4 are used for training. According to the Table 3, mean MSE across these 5 folds shows that generalizability of NN modeling is better than GPR.

Feature importance based on permutation based analysis is also checked in Table 4. This method quantifies each input variable's contribution to model performance by measuring the increase in prediction error when that feature is randomly shuffled while keeping all other features fixed. For each feature in the set $\{Ra, Rb, Ha, MnF, xms, yms\}$, the baseline mean squared error is computed on the training set, then randomly the feature values are permuted and the error is recalculated. This process is repeated 50 times for each feature, and the average increase in error represents the feature's importance score. A large positive score indicates high feature importance, as shuffling it significantly affects model predictions. This model-agnostic method requires no access to the internal model structure. Based on this importance analysis, *Rb* is the most important parameter for each output in both modeling.

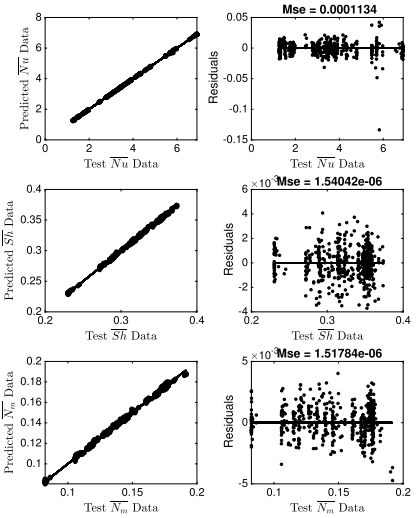

(a) Neural Network results (6.2139 seconds).

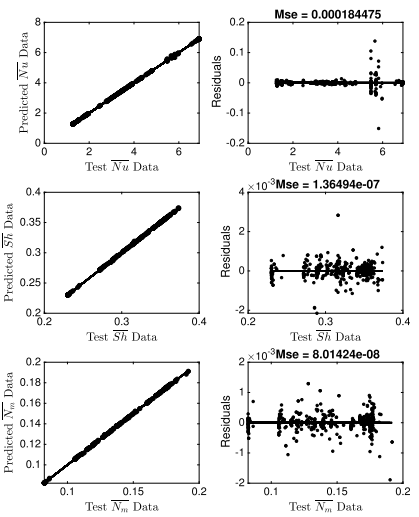

(b) GPR-ARD results (105.79 seconds).

Fig. 2. Comparison of model performance.

Table 3. Cross Validation analysis on $\overline{Nu}$ with both models.

Fold	MSE-NN	MSE-GPR
1	0.000117	0.000413
2	0.000485	0.000347
3	0.000498	0.000567
4	0.000250	0.000359
5	0.000691	0.000739
Mean	0.000408	0.000485

Table 4. Feature importance with both models.

	GPR			NN		
Inputs	$\overline{Nu}$	$\overline{Sh}$	$\overline{Nm}$	$\overline{Nu}$	$\overline{Sh}$	$\overline{Nm}$
Ra	1.9827	0.00152	0.00085	2.2701	0.00159	0.001035
Rb	**3.9684**	**0.00191**	**0.00114**	**4.2053**	**0.00193**	**0.00118**
Ha	0.04015	2.65e-5	7.54e-6	0.0412	2.58e-5	6.59e-6
MnF	1.15e-09	3.90e-17	2.63e-16	8.31e-5	4.15e-8	5.35e-8
xms	0.00423	2.53e-6	1.81e-6	0.00486	2.36e-6	1.72e-6
yms	0.02635	1.37e-5	4.07e-6	0.0275	1.31e-5	3.34e-6

5 Conclusion

In this study, we investigated the prediction capability of two machine learning approaches, NN regression and GPR using the dataset created by the numerical simulation of the natural bioconvection flow of Cu-water nanofluid with oxytactic bacteria in an open square cavity subjected to a magnetic source. The dataset consisting of 2679 convergent solutions was carefully assembled through the RBF method by systematically varying six dimensionless parameters: Ra, Rb, Ha, MnF, xms and yms. The target outputs were the average Nusselt number $\overline{Nu}$, Sherwood number $\overline{Sh}$ and bacteria density $\overline{N_m}$ along the heated wall, each representing a physically meaningful indicator of heat transfer, mass transfer and microbial behavior within the cavity. To ensure that the comparison between the two models was fair and statistically meaningful, we conducted a multi-seed analysis across 31 random seeds, 5-fold cross-validation at a fixed seed, and a permutation-based feature importance analysis. The seed comparison revealed that NN consistently achieves a lower mean MSE, pointing to its stronger predictive accuracy, while GPR-ARD-SE stands out with a noticeably lower standard deviation across seeds, which reflects its robustness and stability regardless of how the data is split. The cross-validation results at seed 28 further supported these findings, with NN attaining a mean MSE of 0.000408 compared to 0.000485 for GPR-ARD, confirming that NN generalizes better to unseen data. The feature importance analysis shows that the bioconvection Rayleigh number Rb emerged as the dominant parameter governing all three output quantities in both models, which is physically consistent given that Rb directly controls the strength of bioconvective flow driven by the density stratification due to bacteria accumulation. Taken together, NN is the preferred choice when prediction accuracy and computational speed are priorities, while GPR-ARD presents itself as a robust and uncertainty-aware modeling framework. Both approaches offer a promising and computationally inexpensive alternative to full numerical simulations.

While the current dataset of 2679 convergent solutions represents a systematic assembled collection, we acknowledge that a larger and more voluminous dataset in broader parameter ranges would further strengthen model generalizability. As future study, broader dataset including higher Hartmann numbers or varying cavity geometries may be collected.

Acknowledgment. This study was supported by TED University Institutional Research Fund (TEDU-IRF) with project ID: T-24-B2010-90130.

References

1. Abdullah, A.A., Rashed, Z.Z.: The stability of bio-thermal marangoni convection in a fluid layer containing oxytactic microorganisms. AIP Adv. **14**(1) (2024)
2. Allouche, S., Djezzar, M., Allouche, B., Tayebi, T.: Magnetohydrodynamic natural convection heat transfer of a nanofluid confined in a square open cavity subjected to a linear varying temperature. Numer. Heat Transfer, Part B: Fundam., 1–23 (2025)
3. Belabid, J., Öztop, H.F.: Nanofluid thermo-bio-convection in a horizontal porous wavy-walled annulus: interaction of phototactic microorganisms and nanoparticles distribution. Int. J. Heat Mass Transf. **215**, 124476 (2023)

4. Biswas, N., Manna, N.K., Mandal, D.K., Gorla, R.S.R.: Magnetohydrodynamic bioconvection of oxytactic microorganisms in porous media saturated with cu-water nanofluid. Int. J. Numer. Methods Heat & Fluid Flow **31**(11), 3461–3489 (2021)
5. Brinkman, H.C.: The viscosity of concentrated suspensions and solutions. J. Chem. Phys. **20**(4), 571–571 (1952)
6. Chan, Y., Tien, C.: A numerical study of two-dimensional natural convection in square open cavities. Numer. Heat Transfer **8**(1), 65–80 (1985)
7. Chandra, P., Das, R.: Finite-element-based machine-learning algorithm for studying gyrotactic-nanofluid flow via stretching surface. Int. J. Numer. Meth. Fluids **95**(12), 1888–1912 (2023)
8. Chow, T.W., Cho, S.Y.: Neural Networks and Computing: Learning Algorithms and Applications, vol. 7, Imperial College Press (2007)
9. Fasshauer, G.E.: Meshfree Approximation Methods with MatLab. World Scientific Publications, Singapore (2007)
10. Fasshauer, G.E., McCourt, M.: Kernel-based Approximation Methods using MATLAB. World Scientific Publications, Singapore (2015)
11. Gangawane, K.M.: Effect of angle of applied magnetic field on natural convection in an open ended cavity with partially active walls. Chem. Eng. Res. Des. **127**, 22–34 (2017)
12. Garnett, J.M.: XII. colours in metal glasses and in metallic films. Philos. Trans. Roy. Soc. London. Ser. A, Containing Pap. Math. Phys. Charact. **203**(359-371), 385–420 (1904)
13. Ghalambaz, M., Mehryan, S., Izapanahi, E., Chamkkha, A., Wen, D.: MHD natural convection of Cu-Al2O3 water hybrid nanofluids in a cavity equally divided into two parts by a vertical flexible partition membrane. J. Therm. Anal. Calorim. **138**, 1723–1743 (2019). https://doi.org/10.1007/s10973-019-08258-w
14. Hill, N., Pedley, T.: Bioconvection. Fluid Dyn. Res. **37**(1–2), 1 (2005)
15. Hussain, S., Öztop, H.F., Alsharif, A.M., Ertam, F.: Mixed bioconvection of nanofluid of oxytactic bacteria through a porous cavity with inlet and outlet under periodic magnetic field using artificial intelligence based on lightgbm algorithm. Therm. Sci. Eng. Progress **50**, 102589 (2024)
16. Kefayati, G., Hosseinizadeh, S., Gorji, M., Sajjadi, H.: Lattice Boltzmann simulation of natural convection in an open enclosure subjugated to water/copper nanofluid. Int. J. Therm. Sci. **52**, 91–101 (2012)
17. Khanafer, K., Vafai, K., Lightstone, M.: Buoyancy-driven heat transfer enhancement in a two-dimensional enclosure utilizing nanofluids. Int. J. Heat Mass Transf. **46**(19), 3639–3653 (2003)
18. Kuznetsov, A.V.: The onset of nanofluid bioconvection in a suspension containing both nanoparticles and gyrotactic microorganisms. Int. Commun. Heat Mass Transfer **37**(10), 1421–1425 (2010)
19. Kuznetsov, A.: The onset of thermo-bioconvection in a shallow fluid saturated porous layer heated from below in a suspension of oxytactic microorganisms. Eur. J. Mech.-B/Fluids **25**(2), 223–233 (2006)
20. Kuznetsov, A.: Nanofluid bioconvection: interaction of microorganisms oxytactic upswimming, nanoparticle distribution, and heating/cooling from below. Theoret. Comput. Fluid Dyn. **26**, 291–310 (2012)
21. Li, H.: Gaussian process regression a machine learning approach to derivative pricing. Ph.D. thesis, Thesis of MSc. Imperial College London (2018)
22. MathWorks, Inc.: MATLAB, Version R2025a. The MathWorks Inc., Natick, Massachusetts (2025). https://www.mathworks.com
23. Mohamad, A., El-Ganaoui, M., Bennacer, R.: Lattice Boltzmann simulation of natural convection in an open ended cavity. Int. J. Therm. Sci. **48**(10), 1870–1875 (2009)

24. Polat, O., Bilgen, E.: Laminar natural convection in inclined open shallow cavities. Int. J. Therm. Sci. **41**(4), 360–368 (2002)
25. Prakash, O., Barman, P., Rao, P., Sharma, R.P.: MHD free convection in a partially open wavy porous cavity filled with nanofluid. Numer. Heat Transfer, Part A: Appl. **84**(5), 449–463 (2023)
26. Rostamian, S.H., Biglari, M., Saedodin, S., Esfe, M.H.: An inspection of thermal conductivity of CuO-SWCNTs hybrid nanofluid versus temperature and concentration using experimental data, ANN modeling and new correlation. J. Mol. Liq. **231**, 364–369 (2017)
27. Sarkar, A., Das, K., Kundu, P.K.: On the onset of bioconvection in nanofluid containing gyrotactic microorganisms and nanoparticles saturating a Non-Darcian porous medium. J. Mol. Liq. **223**, 725–733 (2016)
28. Sezai, I., Mohamad, A.: Suppressing free convection from a flat plate with poor conductor ribs. Int. J. Heat Mass Transf. **42**(11), 2041–2051 (1999)
29. Shafiq, A., Çolak, A.B., Sindhu, T.N.: Significance of bioconvective flow of MHD thixotropic nanofluid passing through a vertical surface by machine learning algorithm. Chin. J. Phys. **80**, 427–444 (2022)
30. Vafaei, M., Afrand, M., Sina, N., Kalbasi, R., Sourani, F., Teimouri, H.: Evaluation of thermal conductivity of MGO-MWCNTS/EG hybrid nanofluids based on experimental data by selecting optimal artificial neural networks. Physica E **85**, 90–96 (2017)
31. Vaferi, B., Samimi, F., Pakgohar, E., Mowla, D.: Artificial neural network approach for prediction of thermal behavior of nanofluids flowing through circular tubes. Powder Technol. **267**, 1–10 (2014)